Strain-Direction-Dependent Growth Morphology of Vicinal Si(001) Surface

C. S. Chang, Y. M. Huang, and Tien T. Tsong
Institute of Physics, Academia Sinica, Nankang, Taipei, Taiwan, Republic of China
(Received 23 May 1996)

The shape dependence of vicinal Si(001) surfaces on the applied uniaxial strain direction is studied. This dependence is intimately related to the anisotropic nature of the intrinsic strain field which originates from the surface dimerization. The strain relief mechanism is shown to be different in two orthogonal directions. Normal to the steps, step-pair bunching and waving lead to formation of hillocks and pits. Along the step direction, bending of step pairs forms a cusp which later develops into a deep groove. [S0031-9007(96)01029-0]

PACS numbers: 68.55.Jk, 68.10.Cr, 68.35.Bs, 68.35.Md

Strain-induced morphological changes of solid surfaces remain an important issue for several decades [1–13]. A nominally flat surface under a uniaxial strain is unstable against the modulation of its shape beyond some critical length. This is known as the Grinfeld instability which has been confirmed experimentally [4–6]. Although this phenomenon should be quite general for any strained system, and was predicted barrierless by continuum models, it has only recently been recognized that strain-induced roughening requires nucleation of steps or facets [14]. This realization is significant and opens up an opportunity to kinetically circumvent some intrinsic adversity in the growth of strain layers. It also points out that a complete understanding of strain-induced surface roughening relies on the unveiling of detailed surface structural characters [13].

One of the details is the effect of reconstruction-induced intrinsic strain field on strain-induced surface roughening, which has long been overlooked. A clean Si(001) surface will undergo reconstruction such that every two Si atoms form a dimer to reduce the unsaturated dangling bonds [15]. As the dimerization occurs, the surface is tensily strained in the dimer bond direction and compressively normal to it, making the intrinsic strain field both anisotropic [16] and long range [17]. Due to the bonding configuration, S_A and S_B steps running in a direction on a reconstructed vicinal Si(001) surface are thus natural stress domain boundaries, and the stripelike strain field deep into the bulk is formed correspondingly. The anisotropy of the strain field is a reflection of that of the steps. When the surface is strained, creation or rearrangement on the steps is thus intimately related to the response of the intrinsic strain field. It is therefore reasonable to suspect the existence of anisotropy in the activation process if the roughening requires nucleation or rearrangement of steps.

In this Letter, we demonstrate that the morphological evolution of vicinal Si(001) surfaces depends on the direction of small applied uniaxial strain, i.e., along or normal to the steps. This dependence, we believe, is a manifestation of the anisotropic response of intrinsic strain field to the applied strain. In addition, the strain-induced or -enhanced phenomena on this surface are observed. These include step bunching and waving, hillocks and/or pits formation, as well as step bending and the development of cusps, which all contribute to surface roughening.

Vicinal Si(001) sample (miscut by $\sim 0.1°$ to $0.3°$) are strained by clamping two ends in length flat to the Ta base plates of unequal height. With this clamping configuration, the portion around the lower end is subjected to compressive strain, and that at the higher end tensile, and the strain gradient along the sample, is roughly constant. Dimensions of our samples are typically $12 \times 2 \times 0.3$ mm^3. A simple estimation shows that maximum strains are applied to the two clamping ends and their magnitudes are $\sim \pm 0.1\%$. The strained sample is then cleaned by repeated flashing to ~ 1230 °C for several times in a pressure of less than 1×10^{-9} Torr, and subsequent annealing at 900 and 650 °C for 2 and 5 min each. Samples with accumulated flashing time longer than 2 min are discarded because a noticeable distortion on the surface usually appears after further cleaning. Once the sample is cooled to room temperature, scanning tunneling microscopy (STM) is used to image the surface. With this sample treatment, the obtained STM images thus represent a quasiequilibrated shape of strained surface covering an estimated range larger than 10 μm [18]. To justify this value, STM images in 5 μm size are taken on several samples while they are heated to ~ 700 °C, and the surface shapes remain the same after a few hours. This implies that the actual equilibrated area is larger than 5 μm and the quasiequilibrium temperature is higher than 700 °C.

The images shown below are reproduced at least twice from different samples under a similar strain. In all the experiments, we find the overall miscut angle in a few μm range is conserved. However, this does not imply the step density is fixed because the up and down steps or wavy steps, generated locally, do not affect the overall miscut angle. Without applied strain, formation of equally spaced steps is stable because "force monopoles"

[17] existing at the adjacent steps repel each other. The net step free energy (E) of the surface per unit length, including the monopole effect, can thus be expressed with two terms: $E = C_1 - C_2 \ln(l/\pi a)$. C_1 is the step formation energy per unit length; C_2 is determined by the surface stress anisotropy, the elastic constants of the medium, and the arrangement of the steps; l is the domain width; a is the lattice constant. This stability is revoked when strain is applied to the surface. The most apparent response of the intrinsic strain field reflects on the size offset of two different domains. In addition, if the strain is applied normal to the step, a second force monopole [19] is created at a step simply due to the discontinuity in height across the step, and its magnitude is proportional to the strain. These step monopoles are attractive to each other, which provides the driving force for step bunching on strained surfaces [20]. Thus, if the strain is sufficiently small such that C_1 in the step free energy formula is not affected and C_2 is only slightly modified, the surface morphology is determined by the interplay of these "force monopoles." If the strain is parallel to the steps, there should be no second force monopole effect.

Step-pair bunching and generation on strained Si(001) surfaces in a 5 μm area are shown in Fig. 1. Several salient features can be noted. Since the uniaxial compressive strain is applied almost normal to the steps, indicated with two arrows, step bunching occurs along this direction also. The wavy nature of the steps is apparent in Fig. 1(a), which is very similar to the results acquired by low energy electron microscopy [21,22] on unstrained Si(001) with miscut angle less than ~0.1°, only here the average miscut angle is ~0.2° by counting the number of steps across the image. Every wave front actually consists of S_A and S_B steps forming a bound pair, with A-type domain dominating, which is more clearly seen in the inset. In the inset, S_B steps are rougher than S_A. Although from one region to another, the spacing among step pairs can vary to 10 times, the width of minority domain does not change accordingly, ranging from ~200 Å in the bunching region to ~300 Å in the region where the step pairs have the widest separation. Also, the step pairs tend to be equally spaced within a region, which reflects the nature of the intrinsic strain field on Si(001). The strain is then calculated to be ~0.03% by converting the areal ratio of domains A and B [17,23]. Strain values given in the following images are estimated in the similar way.

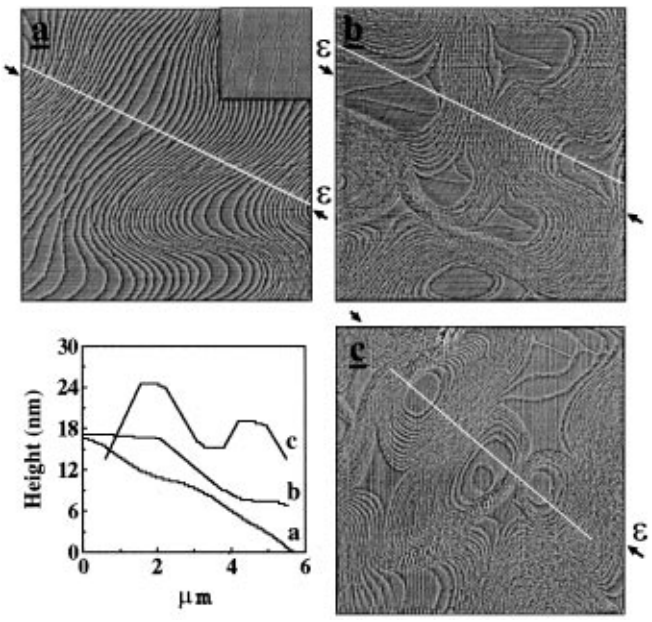

FIG. 1. Flattened STM images (5 μm) showing morphologies of vicinal Si(001) surfaces under uniaxial compressive strains applied perpendicular to the steps. The strain direction is indicated with two arrows. Miscut angle and strain magnitude are (a) ~0.2, ~0.03%; (b) ~0.1°, ~0.02%; and (c) ~0.1°, ~0.03%. The line scans along the white line indicated in each image are displayed to show the comparative surface roughness. The lowest point in the line scan **b** (**c**) has been moved up 7 nm (13 nm). Inset in (a) is an enlarged image taken in one of the bunching regions to show the step pairs. It is also used to define the S_A and S_B steps as well as the direction and sign of the strain.

With a slightly less strain ~0.02% but a smaller miscut angle ~0.1°, the surface shape exhibits new features, as shown in Fig. 1(b). Bunching of step pairs is more evident. A pit has formed, as can be seen at the bottom of the image, which is expected to happen on an unstrained surface only if its miscut angle is less than 0.03° [22]. In Fig. 1(c), the same miscut surface ~0.1° under a strain ~0.03% displays several hillocks and pits. In the formation of hillocks and pits, up and down steps are necessarily created, which result in the increase of surface roughness. The increase in surface roughness is mainly due to a smaller miscut angle (larger average terrace width) by comparing Fig. 1(a) with 1(c).

We have observed a qualitatively similar evolution for the surfaces under tensile strains. From Fig. 1, the pairing of the steps is indeed the most dominant consequence of small applied strains. The morphological changes on this surface should then be considered based on the behavior of step pairs rather than that of single steps. The scale of step-pair bunching and waving on a strained vicinal surface is enhanced when the miscut angle becomes smaller. And with larger strain, bunching is more effective, which leads to easier generation of hillocks and pits on the surface. The evolving trend of the surface shape with the vicinality of the sample and its independence of the sign of strain thus lead us to believe that the character of vicinal Si(001) surface morphologies is still dictated by the intrinsic strain field as long as the magnitude of the applied strain is small. However, even a slight extrinsic strain can induce step-pair bunching and move up the miscut angles which characterize the step waving and the formation of hillocks and/or pits. Therefore, if the strain is applied normal to the steps, the

surface roughening is likely facilitated by step bunching from the extrinsic strain effect and step generation from the intrinsic strain nature.

When the strain is applied parallel to the step direction, the shape response of this surface has a distinctly different character. In Fig. 2 we show images taken under such a condition. The miscut of the samples is $\sim 0.3°$ and the strain applied is tensile except 2(c), where it is compressive. In Fig. 2(a), with small strain $\sim 0.02\%$, the step pairs have already slightly bent in response to the applied strain. The bending creates a small undulation of ~ 2 nm on the surface which can be seen in the line profile below. Since the strain is applied parallel to the steps, there is no driving force for step-pair bunching in the perpendicular direction so that the step pairs are almost equally spaced. The nature of the bending is much more coherent than the waving in Fig. 1. The coherency indicates the existence of a long-range stabilizing field which is most likely to be the intrinsic strain field.

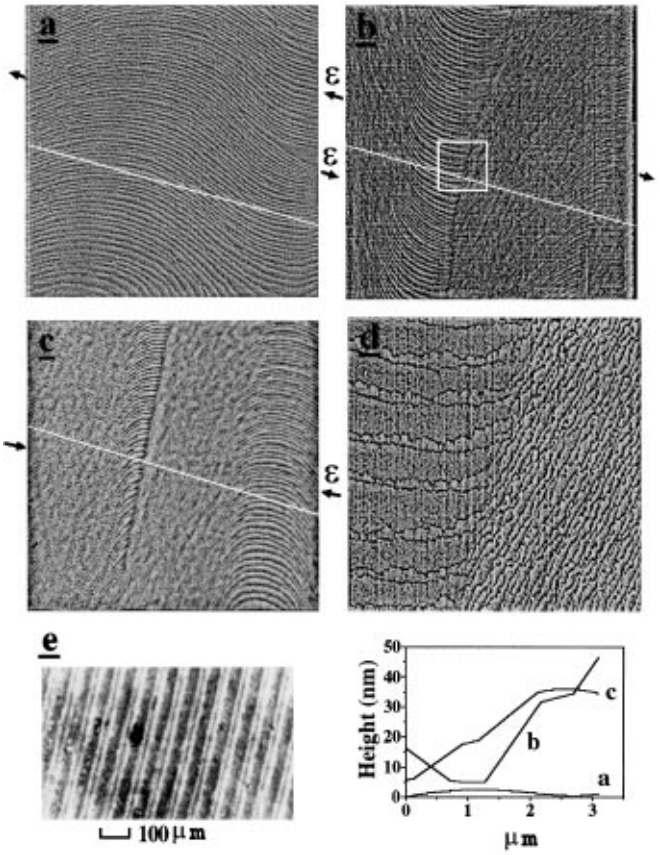

FIG. 2. Flattened STM images (3 μm) showing morphologies of $\sim 0.3°$ miscut Si(001) surfaces under strains applied parallel to the steps. The strain direction is indicated. Strain in (a) $\sim 0.02\%$ tensile, (b) $> 0.02\%$ tensile, and (c) $> 0.03\%$ compressive. (d) Zoom-in image (0.5 μm) of the block in (b) showing the abrupt turns of the steps. (e) SEM image showing deep periodic grooves formed on this surface after prolonged heating. The line scans along the white line indicated in each image are displayed. The lowest points in both **b** and **c** line scans have been moved up 5 nm.

Moving to an area with larger strain, shown in Fig. 2(b), the magnitude of bending increases enormously, which results in a surface undulation of $\sim 20-30$ nm. Referring to the line profile, this image shows only the bottom portion of a cusp. The full cusp here spans $\sim 5-6$ μm. The sharp bending at parts of the steps causes them to appear as a dark line. The zoom-in image at a dark line region, blocked in Fig. 2(b), is shown in Fig. 2(d). Every step pair on the left can be connected to two single steps on the right through an abrupt turn. The dark lines, therefore, mark the distinct boundaries between different stress domains or the singularities of the strain field. The actual strain for this image is not known since it involves strain in the dark line regions. The residual strain estimated from the region having widely spaced step pairs is $\sim 0.02\%$. The dark line regions are very similar to the tips of the cusps described before [12,24]. According to the images here, the cusp can actually contain several such tips. Because of the large surface curvature at a cusp, the accentuation of the strain will proceed at the region, which can later develop into a deep groove after prolong heating. The deep groove can then lead to a crack or other plastic deformations [24]. Scanning electron microscopy images [one of them shown in Fig. 2(e)] taken afterward do show regular deep grooves on the surface for both tensile and compressive strains applied parallel to the steps. Their separations are from a few tens of μm to 100 μm, depending on the magnitude of the strain. Comparing Fig. 2(b) with 2(c), the surface shapes are much alike, which implies the shape does not depend on the sign of applied strain.

Thus, when a small strain is applied parallel to the steps, the surface responds with step-pair bending. As the strain becomes larger, the bending angle gets bigger and steps are crowded in some regions. The strain is then accumulated in the crowd regions and, to some extent, sharp turns are nucleated. The process continues with discrete steps, which then leads to the completion of a full cusp. This behavior is quite different from that seen in Fig. 1. Here, the barrier for generation of new step pairs seems so high that the strain relief has to rely on the large coherent bending of the steps and the nucleation of sharp turns.

So far the strains have all been applied along one of the symmetric axes of the Si(001) surface, i.e., $\langle 100 \rangle$ directions. Strain-induced surface roughening, initiated by either step bunching or bending, should still proceed through some energetically favored pathways. These pathways are closely related to the crystalline structure of the system. One thus would expect to see both strain relief phenomena in almost two orthogonal directions when the strain is applied slightly off the symmetric directions. The result for the sample with one symmetrical

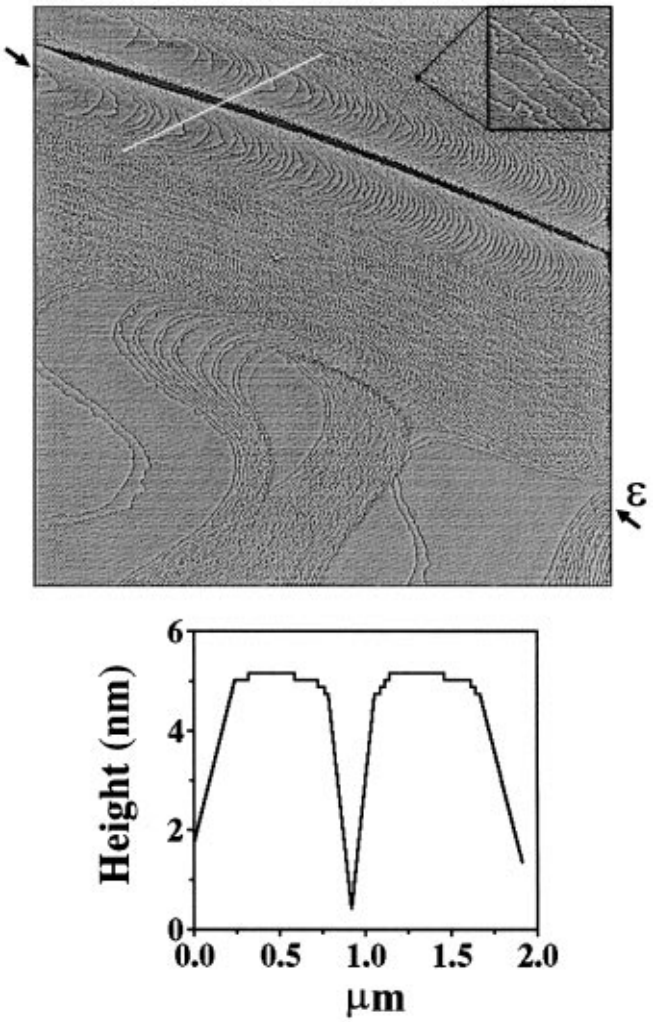

FIG. 3. Flattened STM image (5 μm) of $\sim$0.1° miscut Si(001) surface under an applied compressive strain in a direction 15° off the normal of the steps. Two arrows marked the strain direction. Inset is an image taken in the blocked region having the highest step density, showing dimer rows and unequal domains. The line scan along the white line indicated is displayed to show the height profile of the groove.

axis slanted by $\sim$15° to the strained direction is shown in Fig. 3. The inset is a blowup image taken in the area with the highest step density, indicated with a small block in the figure. It clearly reveals the directions of dimer rows and their associated domains, and no faceting. The surface miscut angle is $\sim$0.1°, and the strain in the bunching direction is $\sim$0.03%. The compressive strain is applied in the direction indicated with two arrows. Step-pair bunching normal to the steps and the sharp depression due to step-pair bending parallel to the steps are both clearly observed.

The authors acknowledge S. U. Jen and Y. Liou for helpful discussions and C. C. Chen for technical assistance and support by National Science Council of the Republic of China under Grant No. NSC85-2112-M-001-039.

[1] J. H. van der Merwe, J. Appl. Phys. **34**, 117 (1963); **34**, 123 (1963).
[2] J. W. Matthews and A. E. Blakeslee, J. Cryst. Growth **29**, 273 (1975); **32**, 265 (1976).
[3] R. J. Asaro and W. A. Tiller, Metall. Trans. **3**, 1789 (1972).
[4] M. A. Grinfeld, Sov. Phys. Dokl. **31**, 831 (1986).
[5] R. H. Torii and S. Balibar, J. Low Temp. Phys. **89**, 391 (1992).
[6] J. Berrehar, C. Caroli, C. Lapersonne-Meyer, and M. Schott, Phys. Rev. B **46**, 13 487 (1992).
[7] D. J. Eaglesham and M. Cerullo, Phys. Rev. Lett. **64**, 1943 (1990).
[8] D. Vanderbilt and L. K. Wickham, in *Evolution of Thin-Film and Surface Microstructure*, edited by C. V. Thompson, J. Y. Tsao, and D. J. Srolovitz, MRS Symposia Proceedings No. 202 (Materials Research Society, Pittsburgh, 1991), p. 555.
[9] C. W. Snyder, B. G. Orr, D. Kessler, and L. M. Sander, Phys. Rev. Lett. **66**, 3032 (1991).
[10] B. J. Spencer, P. W. Voorhees, and S. H. Davis, Phys. Rev. Lett. **67**, 3696 (1991).
[11] F. K. LeGoues, B. S. Meyerson, J. F. Morar, and P. D. Kirchner, J. Appl. Phys. **71**, 4230 (1992).
[12] D. E. Jesson, S. J. Pennycook, J. M. Baribeau, and D. C. Houghton, Phys. Rev. Lett. **71**, 1744 (1993).
[13] Y. H. Xie *et al.*, Phys. Rev. Lett. **73**, 3006 (1994).
[14] J. Tersoff and F. K. LeGoues, Phys. Rev. Lett. **72**, 3570 (1994).
[15] Originated from the fourfold symmetry of the bulk-truncated surface, the reconstructed surface exhibits a rotational degeneracy between the 2×1 (domain A) and 1×2 (domain B) phases. A type-A (type-B) step S_A (S_B) connects an upper 2×1 (1×2) terrace with a lower 1×2 (2×1) terrace. For reference, see D. J. Chadi, Phys. Rev. Lett. **43**, 433 (1979).
[16] F. K. Men, W. E. Packard, and M. B. Webb, Phys. Rev. Lett. **61**, 2469 (1988).
[17] O. L. Alerhand, D. Vanderbilt, R. D. Meade, and J. D. Joannopoulos, Phys. Rev. Lett. **61**, 1973 (1988); V. I. Marchenko, JETP Lett. **33**, 381 (1981).
[18] C. C. Umbach, M. E. Keeffe, and J. M. Blakely, J. Vac. Sci. Technol. A **11**, 1830 (1993); Y. W. Mo, J. Kleiner, M. B. Webb, and M. G. Lagally, Phys. Rev. Lett. **66**, 1998 (1991).
[19] J. Tersoff, Phys. Rev. Lett. **74**, 4962 (1995); Y. H. Xie *et al.*, Phys. Rev. Lett. **74**, 4963 (1995).
[20] J. Tersoff, Y. H. Phang, Zhenyu Zhang, and M. G. Lagally, Phys. Rev. Lett. **75**, 2730 (1995).
[21] J. Tersoff and E. Pehlke, Phys. Rev. Lett. **68**, 816 (1992).
[22] R. M. Tromp and M. C. Reuter, Phys. Rev. Lett. **68**, 820 (1992); Phys. Rev. B **47**, 7598 (1993).
[23] These values are underestimated because the relaxation through surface undulation is not included. Thus, the larger value calculated at a region with wider periodic separation between step pairs seems more reliable. According to the sample clamping geometry, a rough estimation of the strain at the image-taken position along the sample can be a reference to this value.
[24] W. H. Yang and D. J. Srolovitz, Phys. Rev. Lett. **71**, 1593 (1993); D. J. Srolovitz, Acta Metall. **37**, 621 (1989).